Diagn Interv Radiol 2014; 20:168–171

MUSCULOSKELETAL IMAGING
PICTORIAL ESSAY

Clinical, pathological, and imaging characteristics of primitive neuroectodermal tumors of the spine

Hong Guobin, Gu Lingjing, Ding Xianglian, Song Liqing, Peng Hong, Xu Qilan

ABSTRACT
Primitive neuroectodermal tumors (PNETs) located in the spine are extremely rare, and information concerning these tumors in the medical literature is limited to single case reports. This pictorial essay presents the clinical, pathological, and imaging characteristics of PNET of the spine.

Primitive neuroectodermal tumors (PNETs) are malignant tumors thought to arise from the neural ectoderm and comprise undifferentiated small round cells (1–3). PNETs located in the spine are extremely rare, and information concerning these tumors in the medical literature is limited to single case reports (4–5). This pictorial essay presents the clinical, pathological, and imaging characteristics of PNET of the spine.

Clinical features

PNETs are small round cell malignant tumors arising from the neural crest that can be classified as central PNETs (cPNETs) or peripheral PNETs (pPNETs) depending on the site of presentation (1–3). Although pPNET can occur at any age, it is predominant in childhood or adolescents, and its major clinical manifestations involve a soft tissue mass and pain. The prognosis of patients with pPNET is very poor, and the average mortality has been reported to be 70% within three years of diagnosis (6, 7). pPNETs of the spine are extremely rare, with information concerning these tumors being presented in mainly a few case reports (4, 5).

Pathological characteristics

Routine hematoxylin and eosin (H-E) staining and light microscopy manifested uniform, small round tumor cells with little cytoplasm. These cells mainly had round or oval nuclei and were arranged in a pattern of Homer-Wright rosettes. Immunohistochemical staining revealed that three cases were positive for two neural markers, and four cases were positive for three markers (Figs. 1–4).

According to Schmidt et al. (8), the pathological confirmation of PNET must meet the following criteria: the cells display morphological features of malignant, small round cell tumors under a light microscope and are in a pattern of Homer-Wright rosettes; and the tumor cells are positive for at least two neural markers.

Both pPNET and Ewing's sarcoma are known to be composed of small round cells and share similar clinical and pathological features. pPNETs were formally designated by the World Health Organization (WHO) in 1993. In a more recent classification of bone tumors published by WHO in 2002, Ewing's sarcoma and osseous PNET were classified together in one category known as Ewing's sarcoma/PNET (9). PNETs can be distinguished from Ewing's sarcoma due to their neural differences detected by immunohistochemistry. pPNETs express at least two neural differentiation antigens, whereas Ewing's sarcoma expresses only one antigen or sometimes no antigens. In addition, Homer-Wright rosettes can be found in pPNETs but not in Ewing's sarcoma using light microscopy (9, 10).

From the Department of Radiology (H.G. ✉ *honggb2003@163.com*, G.L., D.X., S.L., P.H., X.Q.), Fifth Affiliated Hospital, Sun Yat-sen University, Zhuhai, China; the Department of Radiology (G.L.), Zhuhai People's Hospital, Third Affiliated Hospital, Ji'nan University, Zhuhai, China.

Received 12 February 2013; revision requested 2 April 2013; revision received 9 July 2013; accepted 15 July 2013.

Published online 8 October 2013.
DOI 10.5152/dir.2013.13061

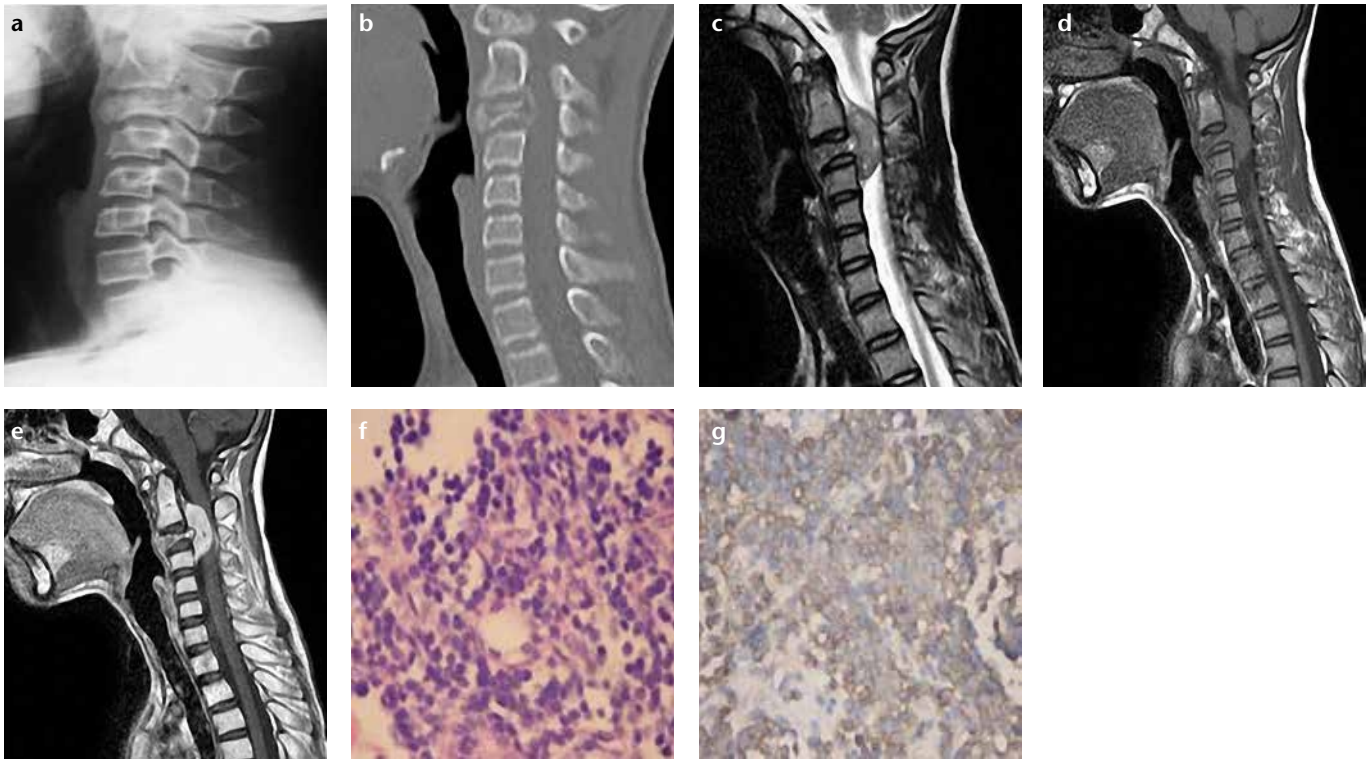

Figure 1. a–g. A 14-year-old male patient with pPNET located in the third cervical vertebra (C3). Lateral projection of the cervical vertebra **(a)** shows compression and flattening of C3 and no narrowing in the neighboring intervertebral space. Sagittal CT **(b)** shows compression and flattening of the C3 vertebra. Sagittal T1-weighted MR image **(c)** and T2-weighted MR image **(d)** show compression and flattening of the C3 vertebra; the soft-tissue mass within the spinal canal (extramedullary) exhibited high and mixed signals on T2-weighted MR images and low signals on T1-weighted MR images. Sagittal contrast-enhanced T1-weighted MR image **(e)** shows a significantly intensified signal of the soft-tissue mass and obvious compression on the spinal cord. Hematoxylin and eosin (H-E) staining (×400) **(f)** shows small round tumor cells, which are closely arranged. Neuron-specific enolase staining (×400) **(g)** shows a positive response.

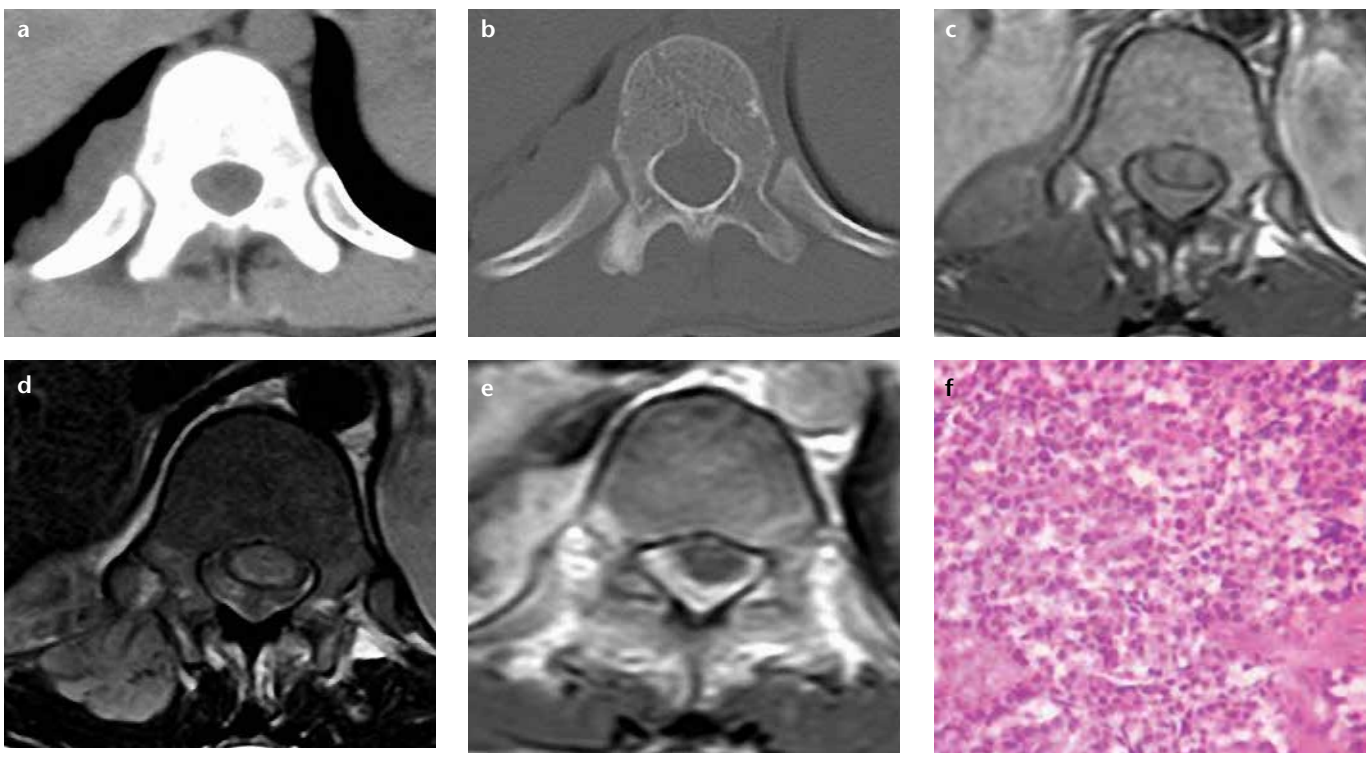

Figure 2. a–f. A 15-year-old male patient with pPNETs located in the thoracic vertebrae. Axial CT **(a, b)** shows osteosclerosis of the right transverse process and the paravertebral soft-tissue mass. Axial T1-weighted MR image **(c)** shows the paravertebral soft-tissue mass and low signals. T2-weighted MR image **(d)** shows high signals. Axial contrast-enhanced T1-weighted MR image **(e)** shows uneven obvious enhancement of the soft-tissue mass. H-E staining (×200) **(f)** shows small round tumor cells, which are arranged closely together.

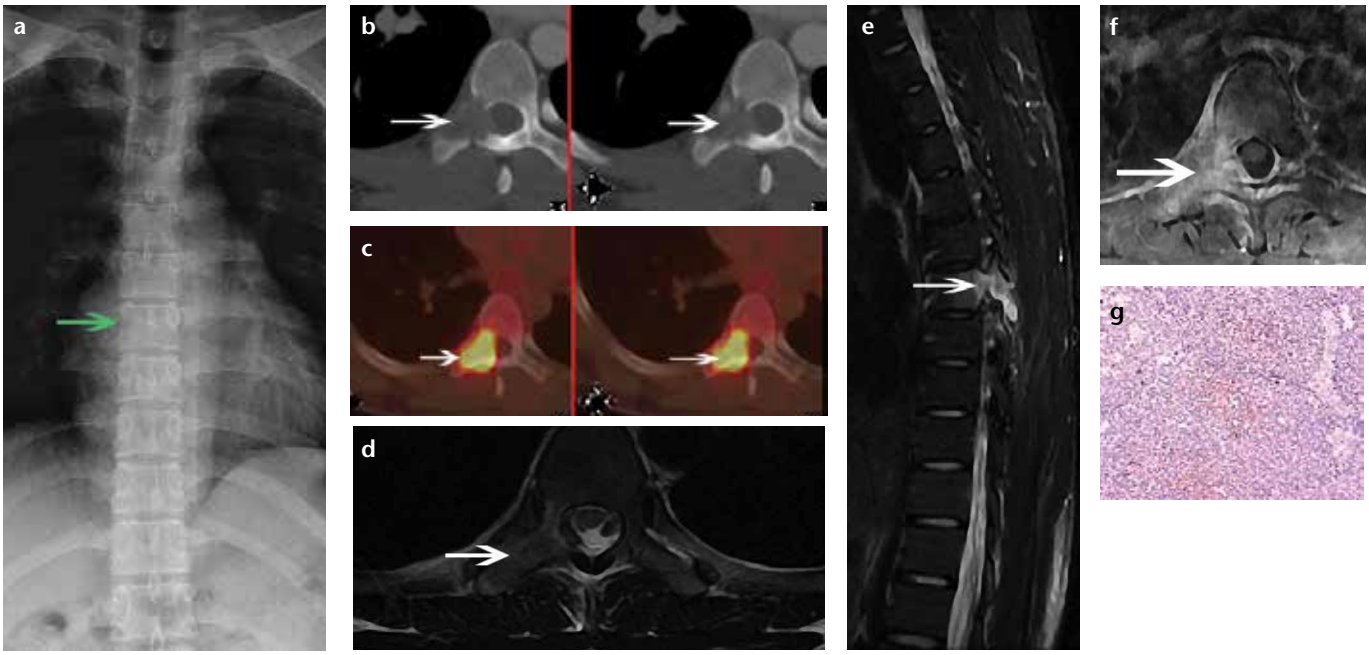

Figure 3. a–g. A 21-year-old male patient with pPNET located in the seventh thoracic vertebra (T7). The X-ray plain film **(a)** shows bone destruction of the right vertebral T7. Axial CT **(b)** shows bone destruction of the right vertebral arch and right transverse process, and the paravertebral soft-tissue mass. Axial positron emission tomography-CT image **(c)** shows a focal fluorodeoxyglucose-avid area (maximum standardized uptake value, 8.8). T2-weighted MR image **(d)** and fat suppression T2-weighted MR image **(e)** show bone marrow signal abnormalities and the paravertebral soft-tissue mass, as well as slightly high signals. Axial contrast-enhanced T1-weighted MR image **(f)** shows uneven obvious enhancement of the lesions. H-E staining (×200) **(g)** shows small round tumor cells, which are closely arranged.

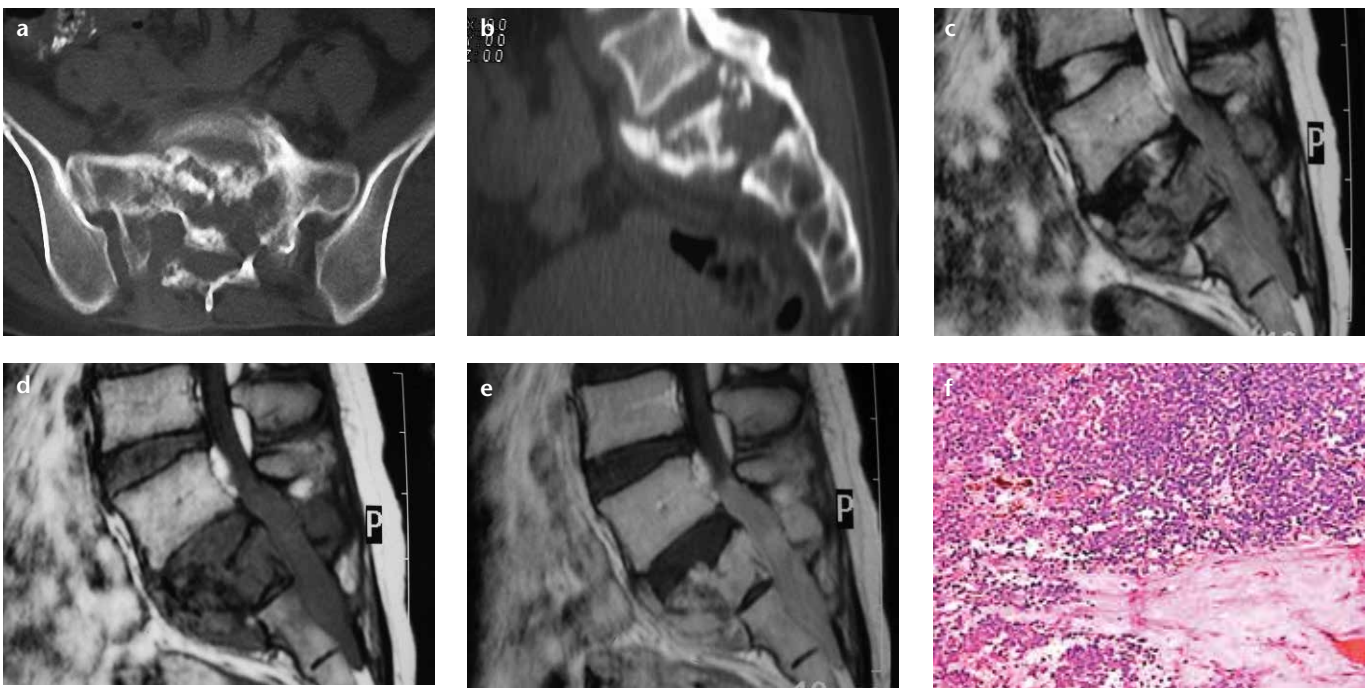

Figure 4. a–f. A 23-year-old female patient with pPNET located in the first sacral vertebra (S1). Axial **(a)** and sagittal **(b)** CT images show bone destruction and osteosclerosis of the S1. MR images **(c, d)** show bone marrow signal abnormalities and the intraspinal soft-tissue mass (extramedullary), as well as slightly high signals on T2-weighted MR image **(c)** and slightly low signals on T1-weighted MR image **(d)**. Sagittal contrast-enhanced T1-weighted MR image **(e)** shows slight enhancement of the lesions. H-E staining (×200) **(f)** shows small round tumor cells, which are arranged closely together.

Imaging findings

Few reports have investigated the imaging characteristics of pPNET of the spine (4, 5, 11, 12). The major imaging features involve bone destruction, a soft tissue mass, uneven signal intensity, and infiltrative growth of the tumor (Figs. 1–4).

Magnetic resonance imaging (MRI) has revealed slightly decreased signal intensity on T1-weighted imaging and slightly increased signal intensity

on T2-weighted imaging, with non-uniform significant enhancement on contrast-enhanced imaging. Moreover, the boundary between the tumor and surrounding tissues is not clearly identified, resulting in difficulty in separation during surgery (4, 13).

Computed tomography (CT) is effective for displaying bone and can also be used to evaluate bone destruction, periosteal reaction, and calcification. Due to high soft-tissue resolution, MRI is useful to show the interior structure of tumors, invasion of adjacent tissues, and distant metastasis.

Thus, CT and MRI play important roles in the evaluation of the interior structure and invasive range of tumors, assessment of the feasibility of surgical excision, and development of the surgical plan, as well as identification of tumor recurrence and metastasis.

Differential diagnosis

It is necessary to distinguish spinal pPNET from eosinophilic granuloma, lymphoma, and metastatic tumors (14). Eosinophilic granuloma mainly occurs in individuals aged less than 20 years and is associated with mild clinical symptoms; the major imaging features include wedge-shaped changes or coin-like lesions in the vertebral body, with less involvement in the accessories or intervertebral disc (14). Lymphoma is usually found in middle-aged and older individuals and is very rare in children aged less than 10 years; the major imaging characteristics involve worm-eaten bone destruction and osteosclerosis, accompanied by an ectosteal soft-tissue mass (14). With a medical history of a primary tumor, metastatic tumors also occur predominantly in middle-aged and older individuals (14). The common manifestations include bone destruction and reactive osteosclerosis, which usually involve the vertebral body and accessories, as well as the presence of a soft-tissue mass.

Conclusion

Spinal pPNET occurs predominantly in children and adolescents. Immunohistochemical staining reveals apparent neural differentiation and positive staining for at least two neural markers, as well as the presence of Homer-Wright rosettes. The imaging features included osteolytic bone destruction and an apparent soft-tissue mass, whereas little evidence exists of periosteal reaction, calcification, or ossification. MRI and CT show the interior structure of tumors and can be used to define the invasive range. In addition, these imaging modalities play a significant role in the identification of the feasibility of surgical excision of the tumors, detection of distant metastasis, and evaluation of the efficacy of therapeutic interventions.

In clinical practice, it is necessary to consider the possibility of pPNET in children and adolescents with osteolytic bone destruction and an apparent soft-tissue mass located in the spine.

Conflict of interest disclosure

The authors declared no conflicts of interest.

References

1. O'Sullivan MJ, Perlman EJ, Furman J, Humphrey PA, Dehner LP, Pfeifer JD. Visceral primitive peripheral neuroectodermal tumors: a clinicopathologic and molecular study. Hum Pathol 2001; 32:1109–1115. [CrossRef]
2. Patnaik A, Mishra S, Mishra S, Deo R. Primary spinal primitive neuroectodermal tumour: report of two cases mimicking neurofibroma and review of the literature. Neurol Neurochir Pol 2012; 46:480–488. [CrossRef]
3. Demir MK, Kosar F, Sanli Y, et al. 18F-FDG PET-CT features of primary primitive neuroectodermal tumor of the chest wall. Diagn Interv Radiol 2009; 15:172–175.
4. Khong PL, Chan GC, Shek TW, Tam PK, Chan FL. Imaging of peripheral PNET: common and uncommon locations. Clin Radiol 2002; 57:272–277. [CrossRef]
5. Cabral GA, Nunes CF, Melo JO Jr, et al. Peripheral primitive neuroectodermal tumor of the cervical spine. Surg Neuro Int 2012; 3:91–91. [CrossRef]
6. Hawkes CP, Betts DR, Obrien J, et al. Congenital sacrococcygeal PNET and chemotherapy. Indian J Med Paediatr Oncol 2012; 33:182–184. [CrossRef]
7. Morris P, Dickman PS, Seidel MJ. Ewing's Sarcoma/Primitive Neuroectodermal tumor of the proximal humeral epiphysis. Orthopedics 2013; 36:e113–116. [CrossRef]
8. Schmidt D, Herrmann C, Jürgens H, Harms D. Malignant peripheral neuroectodermal tumor and its necessary distinction from Ewing's sarcoma. A report from the Kiel Pediatric Tumor Registry. Cancer 1991; 68:2251–2259. [CrossRef]
9. Zhu XZ. Introduction to WHO classification of tumors of bone. J Diag Pathol 2003; 10:201–204.
10. Sanati S, Lu DW, Schmidt E, Perry A, Dehner LP, Pfeifer JD. Cytologic diagnosis of Ewing sarcoma/peripheral neuroectodermal tumor with paired prospective molecular genetic analysis. Cancer 2007; 111:192–199. [CrossRef]
11. Prabu R, Thulkar S, Chand Sharma M, et al. PNET spine: morbid and mortal, but ignored till late. J Pediatr Hematol Oncol 2012; 34:e164–169. [CrossRef]
12. Khong PL, Chan GC, Shek TW, et al. Imaging of peripheral PNET: common and uncommon locations. Clin Radiol 2002; 57:272–277. [CrossRef]
13. Dick EA, McHugh K, Kimber C, Michalski A. Imaging of non-central nervous system primitive neuroectodermal tumors: diagnostic feature and correlation with outcome. Clin Radiol 2001; 56:206–215. [CrossRef]
14. Binning M, Klimo P Jr, Gluf W, et al. Spinal tumors in children. Neurosurg Cli N Am 2007; 18:631–658. [CrossRef]